Journal of General Virology (2016), **97**, 480–486 DOI 10.1099/jgv.0.000354

Short Communication

Marek's disease virus undergoes complete morphogenesis after reactivation in a T-lymphoblastoid cell line transformed by recombinant fluorescent marker virus

Caroline Denesvre,[1] Sylvie Rémy,[1] Laetitia Trapp-Fragnet,[1] Lorraine P. Smith,[2] Sonia Georgeault,[3] Jean-François Vautherot[1] and Venugopal Nair[2]

Correspondence
Caroline Denesvre
denesvre@tours.inra.fr

[1]INRA UMR1282 Infectious Disease and Public Health, ISP, BIOVA team, 37380 Nouzilly, France

[2]Avian Oncogenic Virus Group, The Pirbright Institute, Guildford, GU24 0NF, UK

[3]Département des Microscopies (Plateau Technologique Analyse des Systèmes Biologiques), Université François Rabelais, Tours, France

Received 27 August 2015
Accepted 23 November 2015

T-lymphocytes are central targets of Marek's disease, a major chicken disease induced by the oncogenic alphaherpesvirus Marek's disease virus (MDV). T-lymphocyte infection is also associated with immunosuppression and virus latency. To decipher viral morphogenesis in T-lymphocytes, we used the recombinant vRB-1B 47EGFP marker virus to generate a new lymphoblastoid cell line, 3867K, that exhibited typical properties of other MDV-transformed chicken cell lines in term of cell markers, reactivation rate and infectivity. Examination of reactivating EGFP-positive 3867K cells by transmission electron microscopy revealed the presence of most types of herpesvirus particles inside the cells but no extracellular ones. Quantification of virion types indicated only 5 % cytoplasmic particles, with 0.5 % being mature. This study demonstrated that MDV morphogenesis is complete upon reactivation in T-lymphocytes, albeit with poor efficiency, with a defect in the exit of virions from the nucleus and secondary envelopment, as occurs in infected fibroblasts.

Marek's disease virus (MDV) (species *Gallid herpesvirus 2*) is the causative agent of Marek's disease (MD) in poultry, mostly recognized as malignant T-cell lymphoma. *Gallid herpesvirus 2* is the prototype species of the genus *Mardivirus* within the subfamily *Alphaherpesvirinae*. MDV infection of lymphocytes is characterized by an early acute cytolytic phase during the first week, after which the virus enters latency mostly in $CD4^+$T-cells, a small number of which may become transformed leading to malignant lymphoma. Latently infected lymphocytes, from which virus can be activated, are also believed to be the source of infection to the skin, the unique site from where infectious virus is shed (Calnek, 2001).

Herpesvirus assembly and egress is a complex process (Johnson & Baines, 2011; Mettenleiter, 2002; Mettenleiter *et al.*, 2009; Owen *et al.*, 2015). Particle assembly begins in the nucleus, where the viral genome is packaged into capsids, resulting in type C capsids or nucleocapsids. In most situations, the virions then egress and mature via the double-envelopment mechanism: nucleocapsids exit from the nucleus to the cytoplasm by successive budding into the inner nuclear membrane and subsequent fusion with the outer membrane of primary enveloped virions, which are occasionally visible in the perinuclear space. Finally, the cytosolic nucleocapsids bind several tegument proteins and wrap into Golgi membranes, resulting in mature enveloped virions in vesicles, which are then released from the cell by exocytosis. Only this last type of virion is considered infectious.

Although MDV-infected lymphocytes are usually infectious, visualization of mature enveloped particles by transmission electron microscopy (TEM) in these cells has not been successful (reviewed by Denesvre, 2013). In MD tumour-derived T-lymphoblastoid chicken cell (MDCC) lines, immature particles were visible only in the nucleus as naked capsids or in the perinuclear region as primary enveloped virions (Akiyama & Kato, 1974b; Frazier & Powell, 1975; Nazerian & Witter, 1975). Recently, we reported the presence of cytoplasmic naked capsids in cells explanted from a tumour induced by a partially attenuated MDV strain RB-1B expressing EGFP fused to the N-terminus of the tegument protein, VP22 (vRB-1B EGFPVP22 MDV; Rémy *et al.*, 2013). Our goal here was to visualize the missing cytoplasmic mature virions

in T-cells to measure the efficiency of MDV morphogenesis in T-lymphocytes. For this, our approach was to develop a new MDCC line capable of reactivating EGFP-tagged marker virus to perform qualitative and quantitative TEM analysis.

The MDCC-3867K cell line was obtained from a kidney lymphoma induced by a highly oncogenic recombinant vRB-1B 47EGFP marker virus. This virus expresses the EGFP fused to the C terminus of pUL47, a major tegument protein (Jarosinski *et al.*, 2012). Detailed steps in the establishment of the 3867K cell line have been described elsewhere (Mwangi *et al.* unpublished data). After passage 29, these cells were cultivated at 41 °C in RPMI 1640 supplemented with 10 % FCS, 2 mM glutamine, 10 % tryptose phosphate broth (29.5 g l^{-1}), 4.5 g glucose l^{-1}, 1 % sodium pyruvate and non-essential amino acids. 3867K cells grew in suspension and displayed a polymorphic shape and a heterogeneous size by light microscopy after May–Grünwald–Giemsa (MGG) staining (Fig. 1a). The cytology analysis was evocative of a polymorphic centroblastic lymphoma. Fluorescent *in situ* hybridization analysis with MDV probes indicated that at least six copies of the MDV genome were integrated in the cellular genome of 3867K cells (not shown), confirming their infection by MDV.

Live 3867K cells were examined by flow cytometry on a MoFlo high-speed sorter (Beckman Coulter) in FL1 to detect spontaneous MDV reactivation through the EGFP-tagged pUL47. The results showed that 1–2 % of viable cells spontaneously expressed low levels of EGFP, whereas most cells showed a latent infection and remained EGFP negative (Fig. 1b). MDV-reactivating EGFP-positive cells were selected by cell sorting with a purity of about 88 % (Fig. 1b).

Reverse transcription (RT)-PCR assays were performed on mRNA extracted from EGFP-positive and EGFP-negative sorted 3867K cells as described previously (Trapp-Fragnet *et al.*, 2014) to detect viral gene expression. Late genes such as UL13 and US3 were expressed only in EGFP-positive cells (Fig. 1c). For immediate-early genes like ICP4, RNA expression was observed predominantly in EGFP-positive cells, although some of the EGFP-negative cells also showed low expression, consistent with the previous data on the expression kinetics of early/late genes. The expression of other late antigens was examined using fluorescence microscopy on an Axiovert 200 M inverted epifluorescence microscope equipped with an ApoTome system (Zeiss). 3867K cells were fixed with 4 % paraformaldehyde and stained with a mouse mAb against the capsid VP5 or the tegument VP22 protein plus a secondary fluorescent antibody, as described previously (Blondeau *et al.*, 2007). DNA was stained with Hoechst 33342 (Molecular Probes). VP5 and VP22 were detected in EGFP-positive cells (Fig. 1d), confirming that EGFP-positive cells underwent a lytic cycle.

Examination of 3867K cells after MGG staining (Fig. 1a) and scanning electron microscopy (SEM) (not shown) revealed numerous monobranched extensions at the cell surface. This characteristic was observed previously by SEM on two other MDCC lines, MSB-1 and MOB (Akiyama & Kato, 1974a; Nazerian *et al.*, 1976). However, in the absence of a comparative study on a high number of MDCCs, it is difficult to conclude whether such cell protrusions are a common phenotype of MDCCs. Such cell extensions are atypical for normal avian or human T-cells (Polliack *et al.*, 1973; Stinson & Glick, 1978) and for T-cell lymphomas, including those of MDV origin. Therefore, they may not be directly linked to MD lymphoma development but more directly linked to *in vitro* establishment and/or cultivation of MDCCs. To explore the nature of these protrusions, 3867K cells attached on glass coverslips pre-treated with poly-L-lysine were fixed and their actin filaments labelled with Alexa Fluor 594–phalloidin (Molecular Probes). By fluorescence microscopy, the cells showed cortical actin and projections rich in F-actin at the cell periphery (Fig. 1e). The absence of tubulin and vimentin in these projections (not shown) indicated that they corresponded to filopodia (Mattila & Lappalainen, 2008). Interestingly, most EGFP-positive cells had no, or rare, filopodia at their surface, thus exhibiting a smoother surface than EGFP-negative cells. This difference in the morphology was particularly evident after three-dimensional (3D) reconstitution of images stacks with Imaris sofware (Bitplane) (Fig. 1e). This suggested that a viral determinant expressed during the lytic cycle may induce actin depolymerization interfering with the formation of filopodia. US3, known to induce actin filament breakdown (Deruelle & Favoreel, 2011), is a good candidate for such an effect.

We also observed that 3867K cells could transmit MDV infection at a moderate rate (0.3 %) by co-culture of permissive chicken embryonic skin cell monolayers (not shown). Lastly, flow cytometry revealed that over 98 % of 3867K cells expressed high levels of CD45, MHCII and CD4 but no CD8 or BU1, a B-cell marker (not shown), thus showing that these cells were $CD4^+$ T-lymphocytes, as are most MDCCs. In addition, CD30/Hodgkin's disease antigen, usually expressed on MDCCs, was expressed on only 58.3 % of the 3867K cells and at a low level (not shown). Taken together, these results confirmed that 3867K EGFP-positive cells were infectious upon spontaneous reactivation and constitute an appropriate system to decipher MDV morphogenesis in T-cells at the ultrastructural level.

Therefore, 10^6 EGFP-positive 3867K cells were cell sorted after a pre-treatment of 48 h with 10 μm 5-azacytidine, and were then cultivated overnight for 17 h in the absence of any treatment to allow the potential release of extracellular virions post-sorting. Of note, 5-azacytidine only slightly increased the percentage of reactivated 3867K cells (not shown). Cells were next fixed in Trump's fixative, prepared for TEM and observed on a 1011 microscope (Jeol) as described previously (Rémy *et al.*, 2013). Not all cell sections contained viral particles, as expected from the incomplete cell purification (88 %), with a low number of virions per cell section. When virions were present, their number

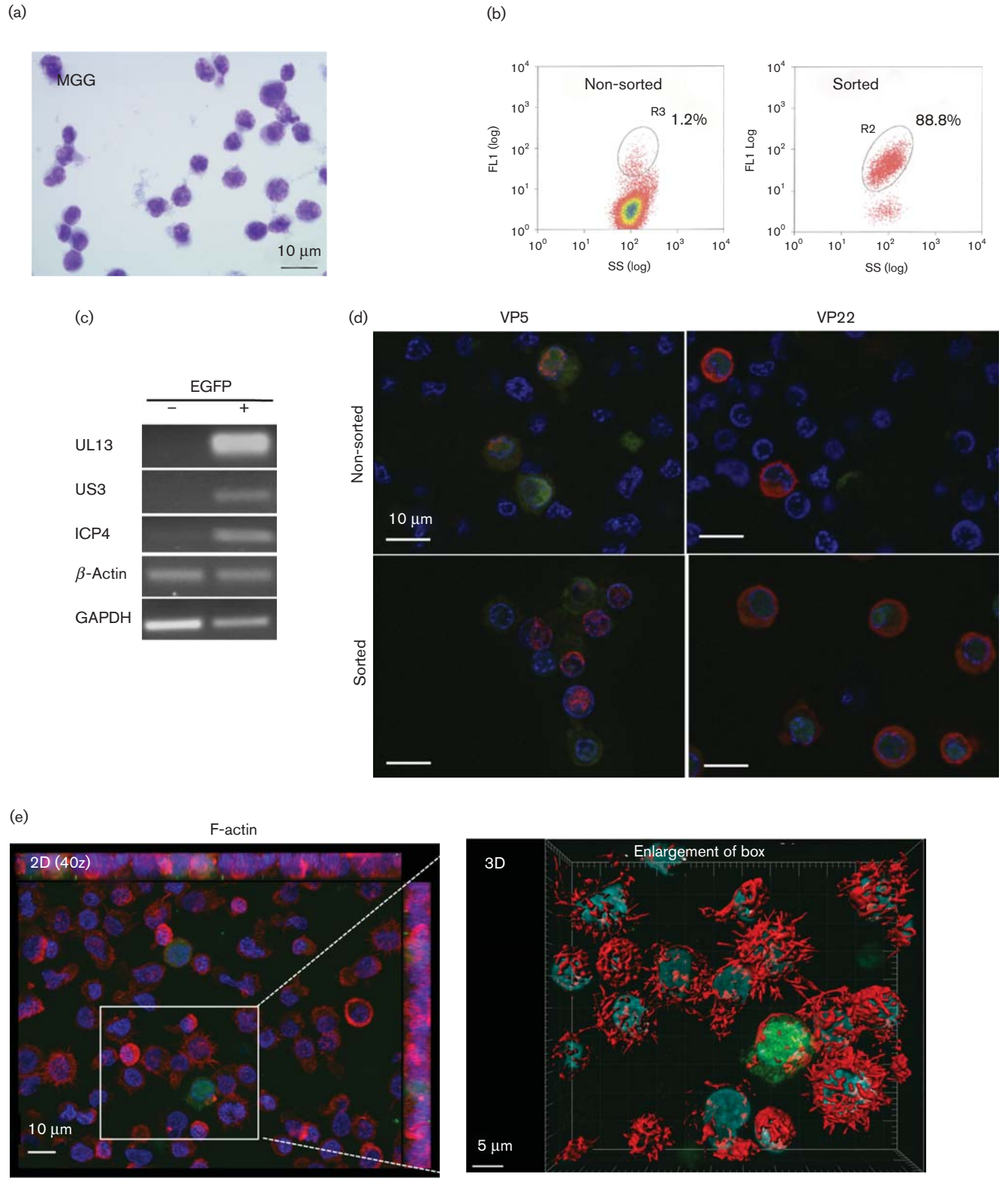

Fig. 1. Morphological and viral characterization of 3867K cells, a new MDCC line induced by vRB-1B EGFP47 MDV. (a) Examination by light microscopy after MGG staining. (b) UL47EGFP was spontaneously expressed in a small proportion of 3867K cells, which were selectable by cell sorting on the basis of EGFP fluorescence, with a yield of 88 %. SS, side scatter. (c) RT-PCR performed on EGFP-positive and -negative sorted cells indicates that EGFP-positive cells expressed various RNAs encoding MDV lytic proteins, such as UL13, US3 and ICP4. (d) EGFP-positive cells, without sorting or after cell

sorting, expressed various MDV lytic antigens (red) detected by fluorescence microscopy. Nuclei were counterstained with Hoechst 33342 (blue) and EGFP was observed directly (co-staining with anti-VP22 or -VP5). (e) F-actin staining with Alexa Fluor 594–phalloidin. Two-dimensional (2D) projections of a 40z stack (left) and three-dimensional (3D) reconstruction (right) showed that filopodia were reduced or absent from EGFP-positive cells but were numerous on most EGFP-negative cells. No EGFP signal was present at the cell surface, indicative of the absence of extracellular virions.

varied from 1 to 21 with a mean of 7.2 (median 6.7) in 120 virion-positive cell sections. All types of particles were unequivocally observed, except for primary enveloped virions and extracellular mature virions. No cells presented all types of virion within the same section (Fig. 2a). The three types of nuclear capsids (A, B and C) were observed (Fig. 2b–d) and were usually scattered in the nucleus. Type C nucleocapsids represented 30.1 % of the total nuclear capsids whereas abortive type A and type B capsids represented 27.2 and 42.6 %, respectively (Table 1). Nuclear virions (96.1 %) were predominant over cytoplasmic ones (3.9 %). Primary enveloped particles were not visualized in the perinuclear space whereas two single capsidless vesicles with a thick membrane were apparent (Fig. 2e). Intracytoplasmic naked capsids were observed only as single particles and were never clustered or associated with electron-dense material. Among the 28 cytoplasmic capsids, we detected seven type A (25 %), two type B (7.1 %) and 19 type C (67.9 %), indicating that nucleocapsids were not the only capsids able to exit from the nucleus (Fig. 2f–h). Partially wrapped or mature enveloped virions were detected, all with a C-type capsid (Fig. 2i, j), but their number represented only 0.5 % of the total virions counted (Table 1). The size of the cytoplasmic enveloped virions was estimated as 153–155 nm and 171–183 nm on two different particles. No structures compatible with extracellular virions or viral biofilm (Pais-Correia *et al.*, 2010) were detected by SEM at the surface of EGFP-positive 3867K cells (not shown), a result in accordance with the absence of an EGFP signal at the cell surface after 3D reconstruction (Fig. 1e).

The novel MDCC-3867K cell line described here was characterized and used as a cell model in order to study MDV morphogenesis in a T-cell context. A large number of MDCC lines have been established in several laboratories since 1973, from various chicken lines and various MDV strains, including a few recombinant tagged viruses (Akiyama & Kato, 1974b; Dienglewicz & Parcells, 1999; Frazier & Powell, 1975; Nazerian, 1987; Nazerian *et al.*, 1977; Parcells *et al.*, 1999; Powell *et al.*, 1974; Schat *et al.*, 1991; Zhao *et al.*, 2011). The 3867K cell line showed numerous characteristics shared by other MDCCs, including cell morphology, cell surface markers, reactivation rate and infectivity, and therefore can be considered as a good MDCC model. In addition, this cell line presents the interesting feature of reactivation of pathogenic EGFP-expressing marker virus, from which cells in the lytic cycle are easily selectable by cytometry.

We were able to unequivocally detect all the morphological types of herpesvirus particles in 3867K cells by TEM, except for the primary enveloped virions. The percentage of the three types of nuclear capsids was comparable to that reported for pseudorabies virus (PRV) (Mettenleiter *et al.*, 1993), indicating the similarities in genome packaging among herpesviruses. Although we did not observe primary enveloped virions, we visualized two perinuclear capsidless vesicles with a morphology very similar to that observed after PRV UL31 and UL34 co-expression (Klupp *et al.*, 2007). The presence of such vesicles suggests that viral-induced budding happens at the inner nuclear envelope in 3867K cells. Therefore, the absence of primary enveloped virions in 3867K is more likely due to a rapid passage of primary enveloped virions through the perinuclear space than to an absence of primary envelopment. However, we observed less than 5 % of the total virions in the cytoplasm, a very low percentage compared with the 30 % levels seen with herpes simplex virus type 1 (Liu *et al.*, 2014). Therefore, the low percentage of cytoplasmic MDV particles in 3867K is in favour of a nuclear egress defect, a phenomenon previously suspected in fibroblasts (Denesvre *et al.*, 2007). In addition, we detected the three types of naked capsid in the cytoplasm, a feature that was also reported in MDV-infected fibroblasts and explanted lymphoma cells with two EGFPVP22 mutants (Rémy *et al.*, 2013). This result confirms that, for MDV, C-type capsids are not the only particles reaching the cytoplasm, as observed for PRV (Mettenleiter *et al.*, 2013), and that for MDV this feature is not cell-type specific or mutant dependent. How nuclear capsids access the cytoplasm is unclear as we did not observe nuclear pore enlargement or nuclear envelope breakdown (Mettenleiter *et al.*, 2013). Comparing the percentage of A-, B- and C-type capsids in the nucleus with the percentage in the cytoplasm indicated, however, a preferential selectivity for C-type capsids. The origin of this inefficient exit of MDV particles from the nucleus remains to be identified. Here, we demonstrated the presence of MDV mature cytoplasmic enveloped particles in reactivating T-cells at low percentage levels similar to fibroblasts. We observed only a few differences between MDV morphogenesis in 3867K cells and in fibroblasts (such as the absence of perinuclear primary enveloped virions and the absence of clusters of naked capsids in the cytoplasm associated with electron-dense material), some of which could be associated with the EGFPVP22 mutant used in fibroblasts. Overall, our study shows that MDV morphogenesis is comparable between the two cell types in terms of virion distribution. Although suspected for a long time because of their capacity to transmit viral infection, this study demonstrates for the first time, to the best of our knowledge, that MDV undergoes

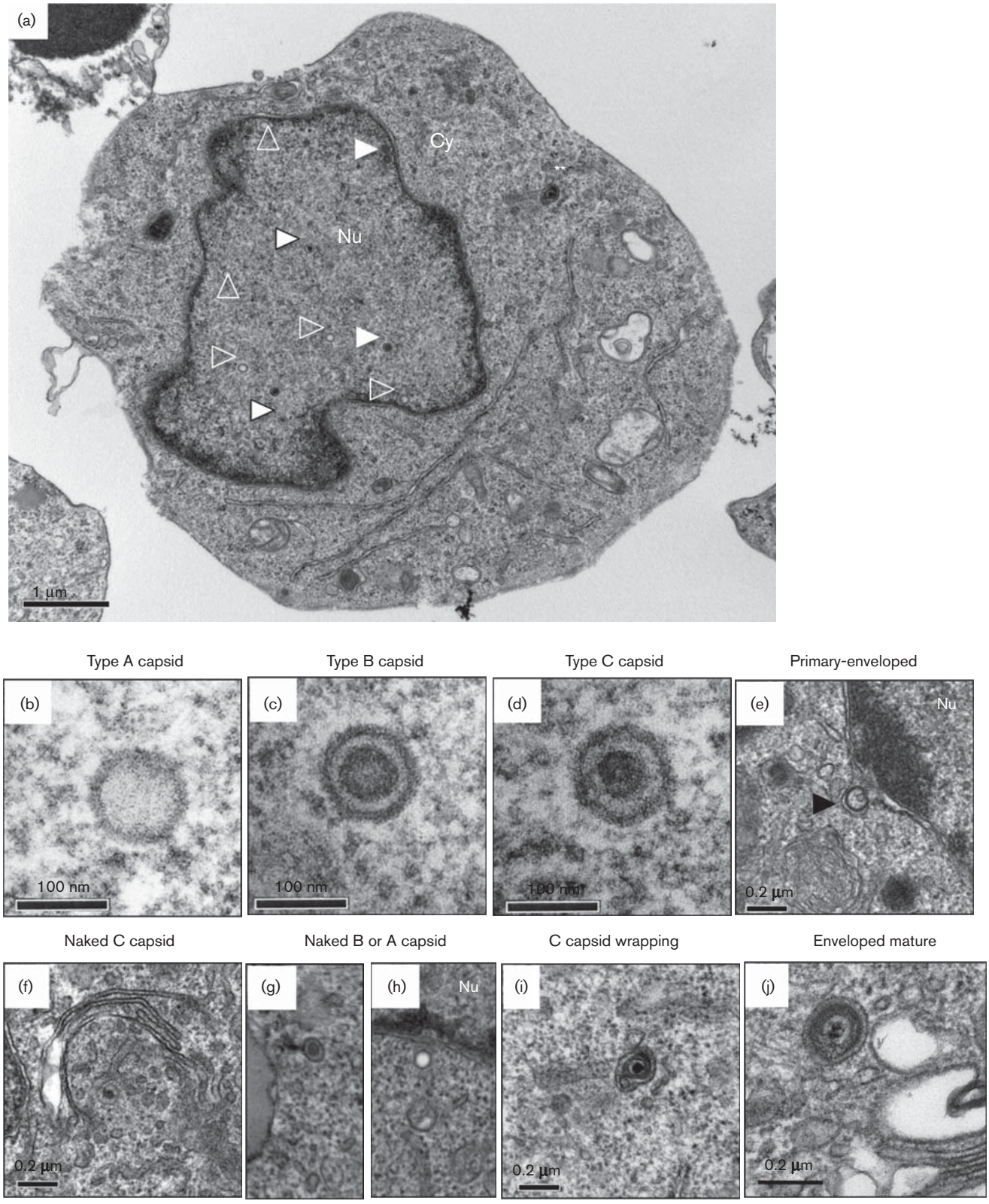

Fig. 2. (a) Overview of EGFP-sorted 3867K cells analysed by TEM. Nuclear capsids are visible as capsid type A (white open triangle), capsid type B (white triangle) and capsid type C (white triangle with a black outline). A C capsid in the process of wrapping (double white asterisks) is shown. Nu, nucleus; Cy, cytoplasm. (b–j) Different types of MDV particles observed by TEM in EGFP-positive sorted 3867K cells. (b–d) The three types of nuclear capsids are shown at high magnification:

type A (b), type B (c) and type C (d). (e) A perinuclear capsidless primary enveloped virion (black triangle) with a thick and smooth electron-dense envelope. (f) A cytoplasmic nucleocapsid surrounded by Golgi stacks. (g, h) Cytoplasmic B-type (g) and A-type (h) capsids. (i) A nucleocapsid in the process of wrapping. (j) A cytoplasmic mature enveloped virion in a vesicle close to membranes.

Table 1. Number and percentages of nuclear, perinuclear and cytoplasmic capsids in virion-positive cells

Total no. of particles counted	No. (%) of nuclear naked capsids			No. (%) of primary enveloped virions	No. (%) of cytoplasmic virions	
	Type A	Type B	Type C		Naked	Mature enveloped
865 (100 %)	226 (27.2 %)	355 (42.6 %)	251 (30.1 %)	1 (0.1 %)	28 (3.2 %)	4 (0.5 %)

Results were determined in 120 virion-positive cell sections.

complete morphogenesis in T-cells, including the final envelopment. The difficulty in deciphering this process until now can be explainable by the low number of these cells undergoing lytic cycle and the rareness of cytoplasmic particles.

Acknowledgements

We thank Julien Gaillard for help with 3D image reconstructions, Yves Le Vern for technical assistance with cytometry, Thibaut Larcher for MGG interpretation and Klaus Osterrieder for the RB-1B 47GFP bacmid. This study has received funding from ERA-NET ANIHWA program 'Marek's Disease Immunosuppression' (grant ANR no. 32000539 to C. D. and grant BBSRC no. BB/L014262/1 to V. N.).

References

Akiyama, Y. & Kato, S. (1974a). Scanning electron microscopy of lymphoid cell lines and lymphocytes from thymus, bursa and blood of chickens. *Biken J* **17**, 193–197.

Akiyama, Y. & Kato, S. (1974b). Two cell lines from lymphomas of Marek's disease. *Biken J* **17**, 105–116.

Blondeau, C., Chbab, N., Beaumont, C., Courvoisier, K., Osterrieder, N., Vautherot, J.-F. & Denesvre, C. (2007). A full UL13 open reading frame in Marek's disease virus (MDV) is dispensable for tumor formation and feather follicle tropism and cannot restore horizontal virus transmission of rRB-1B in vivo. *Vet Res* **38**, 419–433.

Calnek, B. W. (2001). Pathogenesis of Marek's disease virus infection. *Curr Top Microbiol Immunol* **255**, 25–55.

Denesvre, C. (2013). Marek's disease virus morphogenesis. *Avian Dis* **57**, 340–350.

Denesvre, C., Blondeau, C., Lemesle, M., Le Vern, Y., Vautherot, D., Roingeard, P. & Vautherot, J. F. (2007). Morphogenesis of a highly replicative EGFPVP22 recombinant Marek's disease virus in cell culture. *J Virol* **81**, 12348–12359.

Deruelle, M. J. & Favoreel, H. W. (2011). Keep it in the subfamily: the conserved alphaherpesvirus US3 protein kinase. *J Gen Virol* **92**, 18–30.

Dienglewicz, R. L. & Parcells, M. S. (1999). Establishment of a lymphoblastoid cell line using a mutant MDV containing a green fluorescent protein expression cassette. *Acta Virol* **43**, 106–112.

Frazier, J. A. & Powell, P. C. (1975). The ultrastructure of lymphoblastoid cell lines from Marek's disease lymphomata. *Br J Cancer* **31**, 7–14.

Jarosinski, K. W., Arndt, S., Kaufer, B. B. & Osterrieder, N. (2012). Fluorescently tagged pUL47 of Marek's disease virus reveals differential tissue expression of the tegument protein in vivo. *J Virol* **86**, 2428–2436.

Johnson, D. C. & Baines, J. D. (2011). Herpesviruses remodel host membranes for virus egress. *Nat Rev Microbiol* **9**, 382–394.

Klupp, B. G., Granzow, H., Fuchs, W., Keil, G. M., Finke, S. & Mettenleiter, T. C. (2007). Vesicle formation from the nuclear membrane is induced by coexpression of two conserved herpesvirus proteins. *Proc Natl Acad Sci U S A* **104**, 7241–7246.

Liu, Z., Kato, A., Shindo, K., Noda, T., Sagara, H., Kawaoka, Y., Arii, J. & Kawaguchi, Y. (2014). Herpes simplex virus 1 UL47 interacts with viral nuclear egress factors UL31, UL34, and Us3 and regulates viral nuclear egress. *J Virol* **88**, 4657–4667.

Mattila, P. K. & Lappalainen, P. (2008). Filopodia: molecular architecture and cellular functions. *Nat Rev Mol Cell Biol* **9**, 446–454.

Mettenleiter, T. C. (2002). Herpesvirus assembly and egress. *J Virol* **76**, 1537–1547.

Mettenleiter, T. C., Saalmüller, A. & Weiland, F. (1993). Pseudorabies virus protein homologous to herpes simplex virus type 1 ICP18.5 is necessary for capsid maturation. *J Virol* **67**, 1236–1245.

Mettenleiter, T. C., Klupp, B. G. & Granzow, H. (2009). Herpesvirus assembly: an update. *Virus Res* **143**, 222–234.

Mettenleiter, T. C., Müller, F., Granzow, H. & Klupp, B. G. (2013). The way out: what we know and do not know about herpesvirus nuclear egress. *Cell Microbiol* **15**, 170–178.

Nazerian, K. (1987). An updated list of avian cell lines and transplantable tumours. *Avian Pathol* **16**, 527–544.

Nazerian, K. & Witter, R. L. (1975). Properties of a chicken lymphoblastoid cell line from Marek's disease tumor. *J Natl Cancer Inst* **54**, 453–458.

Nazerian, K., Ackerson, A. & Hooper, G. (1976). Scanning electron microscopy in the study of chicken T and B cells and cells from Marek's disease tumours. *Avian Pathol* **5**, 135–145.

Nazerian, K., Stephens, E. A., Sharma, J. M., Lee, L. F., Gailitis, M. & Witter, R. L. (1977). A nonproducer T lymphoblastoid cell line from Marek's disease transplantable tumor (JMV). *Avian Dis* **21**, 69–76.

Owen, D. J., Crump, C. M. & Graham, S. C. (2015). Tegument assembly and secondary envelopment of alphaherpesviruses. *Viruses* **7**, 5084–5114.

Pais-Correia, A. M., Sachse, M., Guadagnini, S., Robbiati, V., Lasserre, R., Gessain, A., Gout, O., Alcover, A. & Thoulouze, M. I. (2010). Biofilm-like extracellular viral assemblies mediate HTLV-1 cell-to-cell transmission at virological synapses. *Nat Med* **16**, 83–89.

Parcells, M. S., Dienglewicz, R. L., Anderson, A. S. & Morgan, R. W. (1999). Recombinant Marek's disease virus (MDV)-derived lymphoblastoid cell lines: regulation of a marker gene within the context of the MDV genome. *J Virol* **73**, 1362–1373.

Polliack, A., Lampen, N., Clarkson, B. D., De Harven, E., Bentwich, Z., Siegal, F. P. & Kunkel, H. G. (1973). Identification of human B and T lymphocytes by scanning electron microscopy. *J Exp Med* **138**, 607–624.

Powell, P. C., Payne, L. N., Frazier, J. A. & Rennie, M. (1974). T lymphoblastoid cell lines from Marek's disease lymphomas. *Nature* **251**, 79–80.

Rémy, S., Blondeau, C., Le Vern, Y., Lemesle, M., Vautherot, J.-F. & Denesvre, C. (2013). Fluorescent tagging of VP22 in N-terminus reveals that VP22 favors Marek's disease virus (MDV) virulence in chickens and allows morphogenesis study in MD tumor cells. *Vet Res* **44**, 125.

Schat, K. A., Chen, C. L., Calnek, B. W. & Char, D. (1991). Transformation of T-lymphocyte subsets by Marek's disease herpesvirus. *J Virol* **65**, 1408–1413.

Stinson, R. & Glick, B. (1978). Scanning electron microscopy of chicken lymphocytes: a comparative study of thymic, bursal, and splenic lymphocytes. *Dev Comp Immunol* **2**, 311–318.

Trapp-Fragnet, L., Bencherit, D., Chabanne-Vautherot, D., Le Vern, Y., Rémy, S., Boutet-Robinet, E., Mirey, G., Vautherot, J. F. & Denesvre, C. (2014). Cell cycle modulation by Marek's disease virus: the tegument protein VP22 triggers S-phase arrest and DNA damage in proliferating cells. *PLoS One* **9**, e100004.

Zhao, Y., Xu, H., Yao, Y., Smith, L. P., Kgosana, L., Green, J., Petherbridge, L., Baigent, S. J. & Nair, V. (2011). Critical role of the virus-encoded microRNA-155 ortholog in the induction of Marek's disease lymphomas. *PLoS Pathog* **7**, e1001305.